

## Chapter 5

# Dynamic Crack Propagation in Layered Transparent Materials Studied Using Digital Gradient Sensing Method: Part-II

Balamurugan M. Sundaram and Hareesh V. Tippur

**Abstract** Dynamic fracture behavior of bi-layered PMMA samples are studied using Digital Gradient Sensing (DGS) in conjunction with high-speed photography. DGS exploits elasto-optic effect exhibited by transparent solids subjected to a non-uniform state of stress causing deflection of light rays propagating through the material. The current work builds on authors' previous report concerning crack trapping, interfacial bifurcation, and mixed-mode penetration into the second layer when a dynamically growing mode-I crack in the first layer encounters a normally oriented interface of different strengths. The current work specifically focuses on the role of the interface location within the bi-layered specimen relative to the initial crack tip on fracture behavior with an intention of examining the effect of the incident crack speed and the associated stress intensity factors for select interfacial fracture toughness. The location of the interface is varied sequentially from 'near' to 'far' from the initial notch tip to accomplish this task. Preliminary results suggest that crack growth in both the interface and the second layer are greatly affected by the location of the interface. That is, the velocity and stress intensity factors of the incident crack affect the outcome of the overall fracture behavior of bi-layered samples including interfacial trapping and penetration into the second layer.

**Keywords** Digital gradient sensing • Transparent material • Layered material • Dynamic fracture • Crack path selection

## 5.1 Introduction

Optically transparent, impact resistant materials are used in various aerospace, automotive and military applications as windshields, protective canopy, face-shields, etc. In these applications, layered material architectures are routinely employed (e.g., safety or laminated glass). The ability of such materials to bear load and structurally survive impact loading is critical, especially when human lives and mission critical instruments are involved. Hence, it is essential that the mechanical failure characteristics of transparent materials and structures under impact loading conditions are well understood.

Many works reported in the literature focus on crack-interface interactions involving a growing crack and an inclined interface [1], resulting in a dominant penetrated crack in the subsequent layer following interfacial crack growth. Yet, relatively few reports exist on a more common and practical scenario of growing cracks interacting with normally oriented interfaces [2]. Accordingly, this work investigates the fracture response of an elastically homogeneous PMMA bi-layer with a discrete plane of weakness. The goal here is to study the fracture response when dynamically growing cracks of different velocity and stress intensity factor reach an interface oriented *perpendicularly* to the crack growth direction. The stress intensity factor evaluation is accomplished by using an optical technique called Digital Gradient Sensing in conjunction with high-speed photography. This study is a continuation of the previous work by the authors on the same material system/geometry with different interfacial fracture toughness. In this study the effect of the position of the layer within the geometry is studied. Of particular interest are dynamic crack deflection, bifurcation and penetration mechanisms across an interface located in the path of a dynamically propagating crack when the interface location is varied.

## 5.2 Digital Gradient Sensing

Full-field optical measurement techniques are preferable to point-wise methods in fracture and failure studies. In recent years, digital image correlation (DIC) has become increasingly popular as they require ordinary white light illumination, relatively simple optics, digital electronics and little/no surface preparation. With the introduction of ultrahigh-speed digital

---

B. M. Sundaram • H.V. Tippur (✉)  
Department of Mechanical Engineering, Auburn University, Auburn, AL 36849, USA  
e-mail: [htippur@eng.auburn.edu](mailto:htippur@eng.auburn.edu)

cameras, DIC has been extended to study transient problems [3] including dynamic fracture. In this context, a technique called Digital Gradient Sensing (DGS) [4] that employs 2D DIC for quantifying elasto-optic effects in transparent materials has been introduced. The optical measurements in this method represent two orthogonal in-plane stress gradients under plane stress conditions and offer several advantages for studying transparent materials.

In transmission-mode DGS [4] a speckle decoration on a planar surface, called the ‘target’, is photographed through a planar, optically transparent sheet under investigation. White light illumination is used for recording gray scales on the target. The speckle pattern is first photographed through the specimen in its undeformed state to record a reference image. Upon loading, the non-uniform stresses due to the applied loads change the local refractive index. Additionally, the Poisson effect produces a non-uniform thickness change. A combination of these, commonly known as the *elasto-optic effect*, cause the light rays to deviate from their initial path. The speckle pattern is once again photographed through the specimen in this deformed state. The local deviations of light rays can be quantified by correlating speckle images belonging to deformed and reference states to find displacement components. Under paraxial approximations, the angular deflections of light rays in two orthogonal planes ( $x$ - $z$  and  $y$ - $z$  planes with  $z$ -axis coinciding with the optical axis of the setup and  $x$ - $y$  being the specimen plane coordinates) can be computed using these displacement components if the distance between the specimen plane and the target plane is known. A detailed analysis (see, [4]) suggests that the local angular deflections are related to the gradients of in-plane normal stresses as,

$$\phi_x = C_\sigma B [\partial(\sigma_x + \sigma_y)/\partial x], \phi_y = -C_\sigma B [\partial(\sigma_x + \sigma_y)/\partial y] \quad (5.1)$$

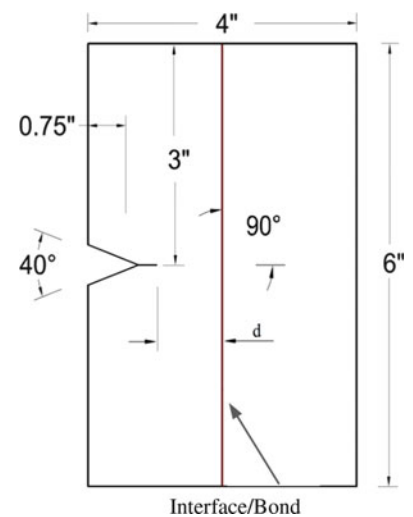
where  $C_\sigma$  is the elasto-optical constant of the material and  $B$  is its thickness.

### 5.3 Specimen Geometry and Preparation

The bi-layered specimens with interface normally oriented to the prospective crack growth direction were prepared by bonding two cast PMMA sheets using a commercially available acrylic adhesive to form a rectangular layered material system of approximate dimension  $6'' \times 4''$  and thickness  $\times 0.33''$ . The interfacial fracture toughness of interface (100  $\mu\text{m}$  thick) was [5] approximately 50 % of the virgin PMMA ( $\sim 1.3 \text{ MPa}\sqrt{\text{m}}$ ). By varying the position of the interface with respect to the initial crack tip, various specimen configurations were obtained. Figure 5.1 shows the different specimen configurations used in this work.

The specimen preparation involved sanding the bond surfaces using 400 grit sand paper. The adhesive was applied to one of the two surfaces and both the surfaces were squeezed against each other using a bench-vise. A spacer of 100  $\mu\text{m}$  thickness was placed between the two layers to control the interface thickness [5]. This was repeated for various interface positions. At least two specimens of each configuration were prepared to check experimental repeatability.

**Fig. 5.1** Bi-layered material system with a normally oriented interface. The distance ‘d’ = 9 mm, 17 mm, 28 mm and 42 mm were used.



## 5.4 Experimental Details

The schematic of the experimental setup used for dynamic fracture tests is shown in Fig. 5.2. The setup included a 6 ft long, 1 in. diameter long-bar with a wedge shaped tip held against the unconstrained specimen with an identical wedge shaped notch and a 12 in. long, 1 in. diameter striker held inside the barrel of a gas-gun. Both the long-bar and the striker were of the same diameter and made of aluminum 7075 to eliminate the impedance mismatch between them. The striker was launched towards the long-bar using the gas-gun at a velocity of  $\sim 14$  m/s. When the striker contacted the long-bar, a compressive stress wave propagated along the bar before transmission into the specimen in contact.

A target plate with random black and white speckles was placed behind the specimen at a fixed distance ( $\sim 25$  mm) to measure deformations using DGS. The speckle pattern was photographed through the specimen using a Cordin-550 ultrahigh-speed digital camera. It has 32 independent CCD image sensors positioned radially around a rotating mirror which sweeps image over these sensors. Prior to loading, a set of 32 reference images were recorded at a rate of  $\sim 200,000$  frames per second at a resolution of  $1000 \times 1000$  pixels per image. When the striker contacted the long-bar, a trigger signal initiated recording of a second set of 32 images at the same framing rate recording the fracture event.

Thus each reference image had a corresponding deformed image. The corresponding reference and deformed images from same sensor were paired. The paired sets of images were then correlated to obtain in-plane displacements before evaluating angular deflections of light rays at a 2-D array of spatial positions in the field of view.

## 5.5 Crack Path Selection

In Fig. 5.3a–d the ‘V’ notch is extended using a diamond impregnated blade to form the initial crack tip. The crack growth occurs from left to right in these photographs. There is a single crack initiated at the crack tip in layer-I which is predominantly mode-I in nature. In Fig. 5.3a it can be seen that when the interface at  $\sim 9$  mm from the initial crack tip a

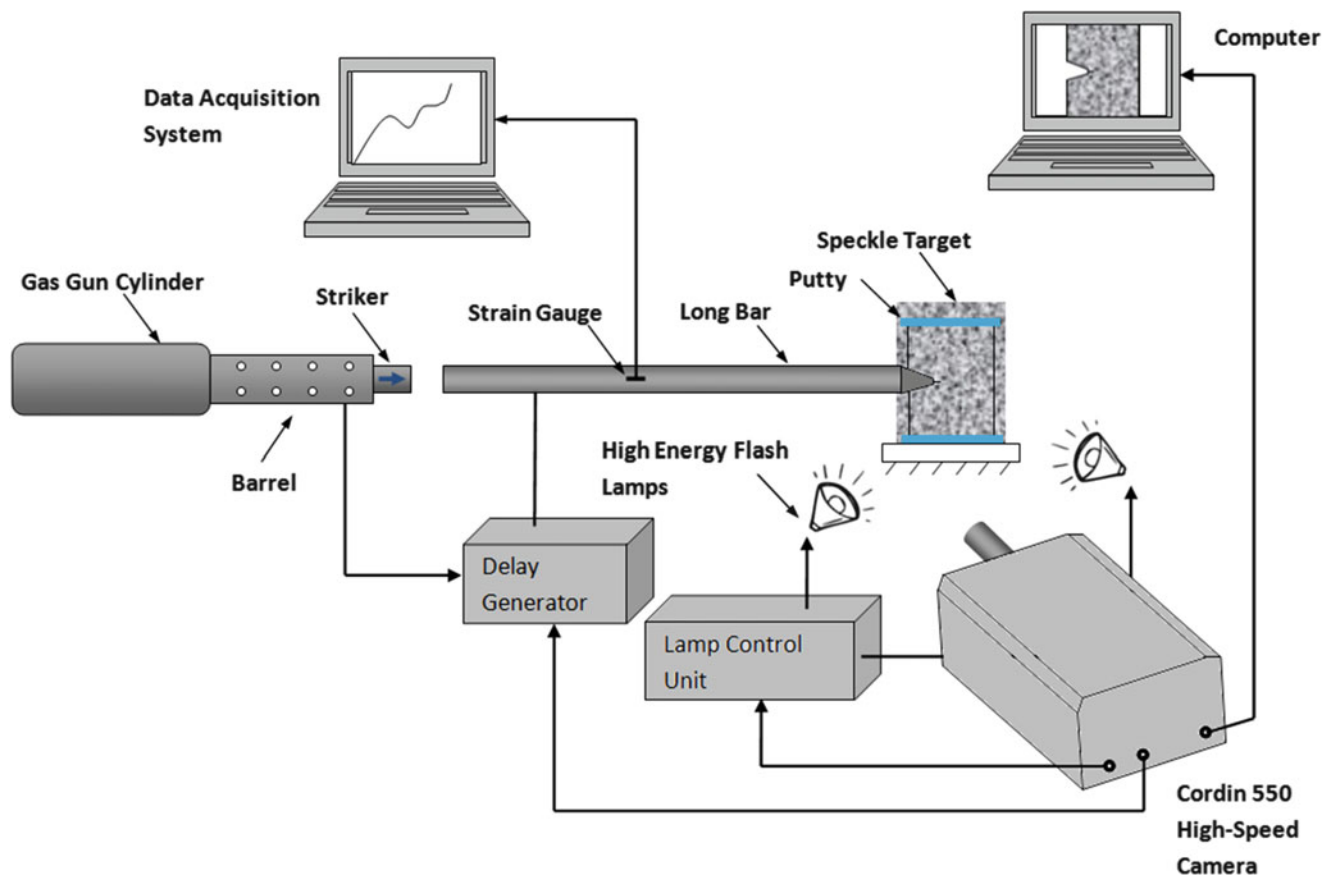
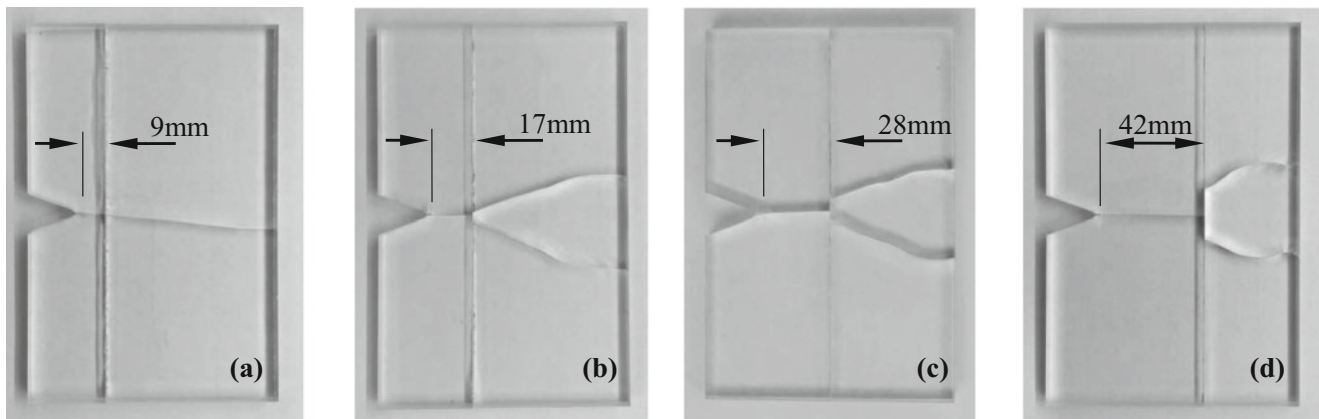
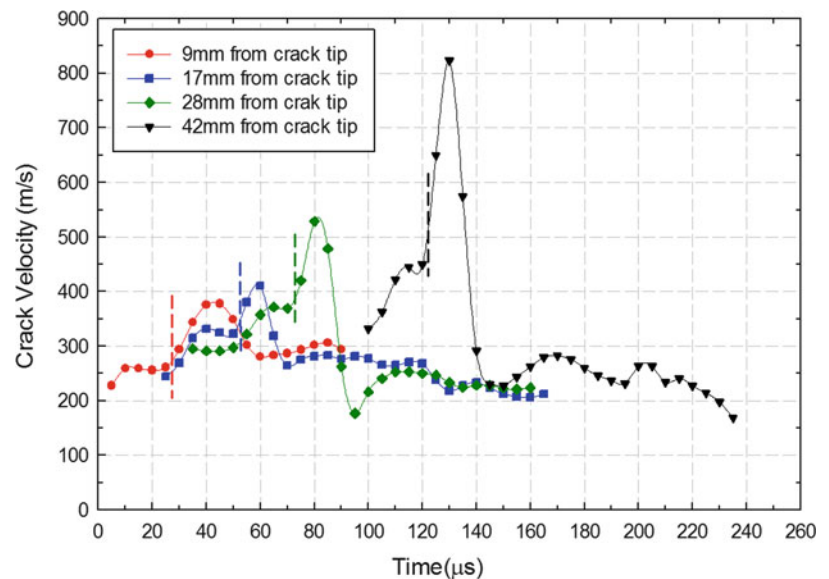


Fig. 5.2 Schematic of the experimental setup



**Fig. 5.3** Photographs of fractured specimens showing crack path (growth from *left to right*) selection upon interacting with a normal weak interface. The incident crack speed for different interface locations differ.

**Fig. 5.4** Crack velocity histories for different interfacial locations in the samples. *Dotted vertical line* represent the approximate time at which the crack reaches the interface.



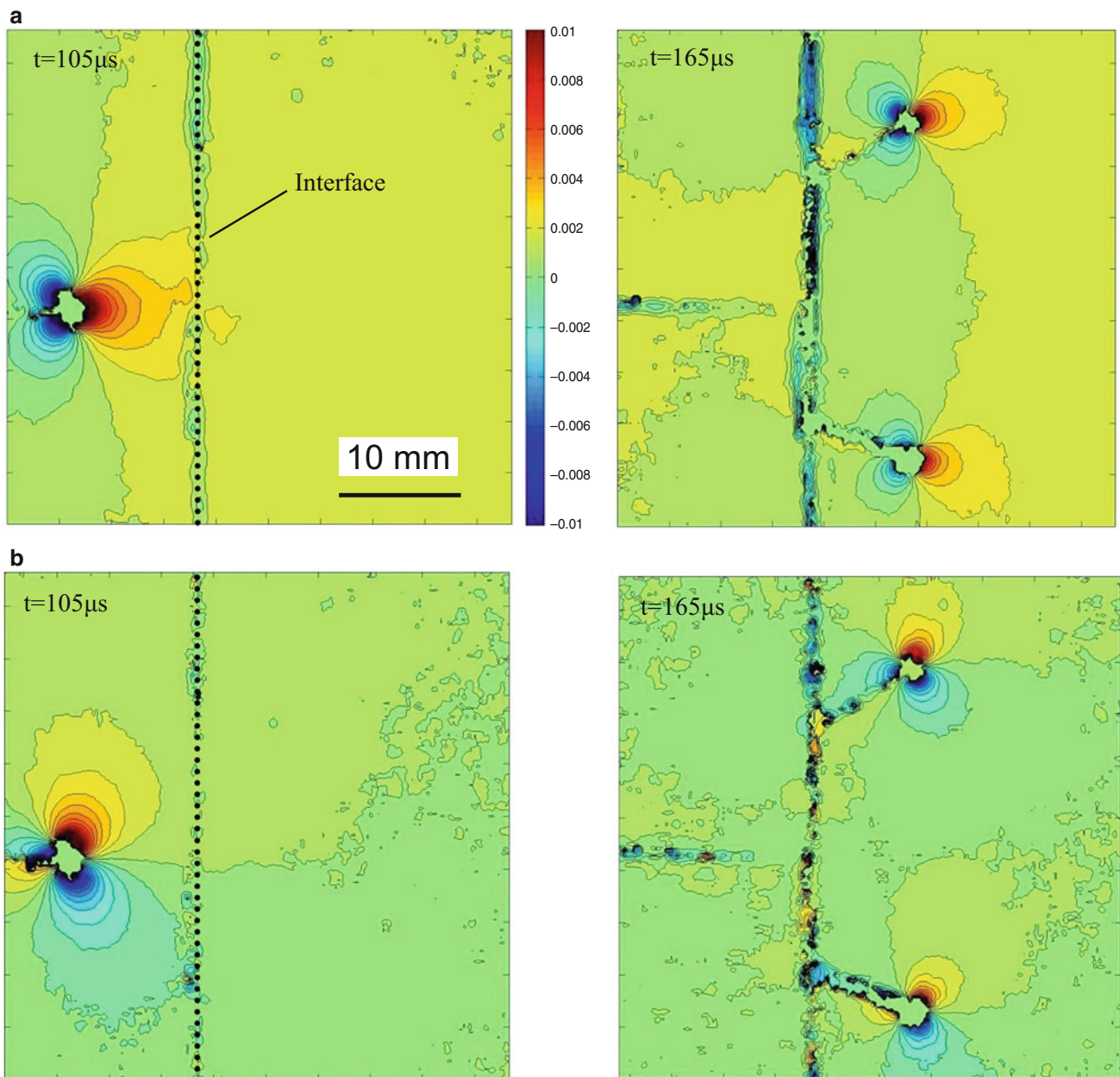
single crack emerges into the layer-II which is also predominantly mode-I type. On the other hand, in Fig. 5.3b–d two complex growth patterns involving crack bifurcation and interfacial crack growth followed by mixed-mode penetrated crack branches in layer-II can be seen. The two daughter cracks produced in layer-II travel symmetrically (relative to the specimen configuration) throughout their propagation. It can be seen that the distance travelled by the two daughter cracks in the interface were 2, 12, 22 mm for interface positions of 17, 28 and 42 mm, respectively. There is a clear evidence of increase in interfacial trapping/crack growth as the interface is located further away from the initial crack tip. There is also evidence of different crack angles at crack penetration into layer-II.

Figure 5.4 shows plots of crack velocity histories for all the four configurations. It can be seen that all the configurations show similar crack growth patterns in terms of velocity histories. In each configuration, the velocity when the crack impinges on the interface is different. There is a noticeable increase in the velocity when the crack approaches the interface. The increase in the distance of the interface from the initial notch also produces an increase incident velocity. From this, one could infer that the velocity of the crack when it impinges on the interface is a key factor in the subsequent interfacial bifurcation, and penetration/branching mechanisms observed. It should also be noted that the final crack velocity observed in layer-II in case of farthest interface (42 mm) from the initial crack tip is the lowest (~160 m/s) compared to the other configurations (~300 m/s for the 9 mm case). Furthermore, the crack speed reached by the bifurcated cracks within the

interface also attain higher values when the interface is situated farther away from the initial notch tip or the incident crack velocity is higher ( $>800$  m/s vs.  $<400$  m/s in the 42 mm vs. 9 mm cases, respectively). This is a rather counterintuitive observation that needs further investigation.

## 5.6 Optical Measurements

The recorded reference and deformed images were correlated using ARAMIS™ to obtain contours of constant angular deflections near a propagating crack tip. The details are avoided here for brevity. The resulting contours in Figs. 5.5 and 5.6 represent the angular deflections of light rays in various configurations (42mm and 9mm respectively) and represent the



**Fig. 5.5** Angular deflection contour plots proportional to stress-gradients in the  $x$ - and  $y$ -directions for an interface at 42 mm from initial crack tip. (a)  $\phi_x$  contour. (b)  $\phi_y$  contours

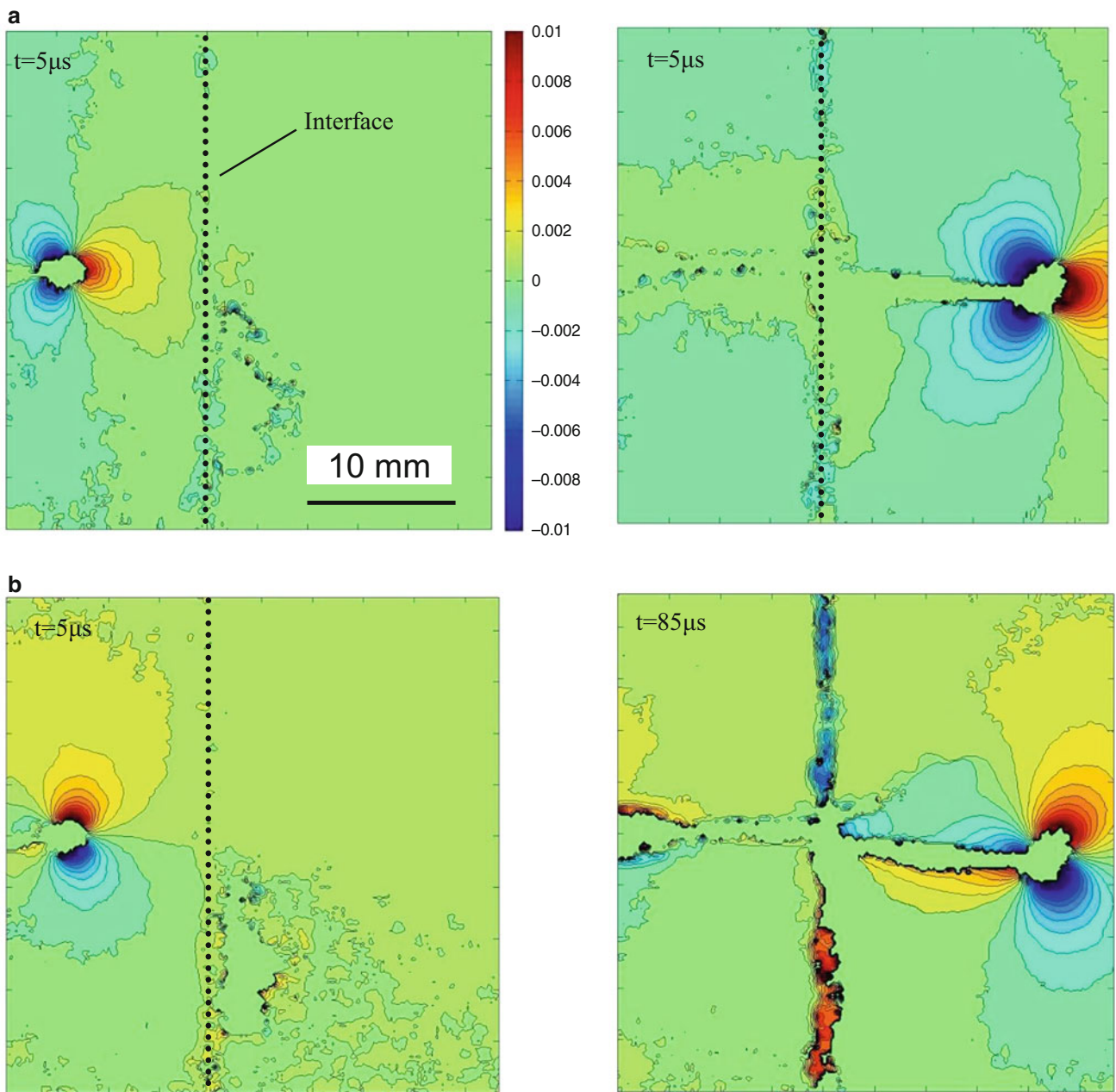


**Fig. 5.6** Angular deflection contour plots proportional to stress-gradients in the  $x$ - and  $y$ -directions for an interface at 9 mm from the initial crack tip. (a)  $\phi_x$  contours (b)  $\phi_y$  contours

stress gradients [5] in two mutually perpendicular directions. Here only few representative plots for a few select cases are shown and  $t = 0 \mu s$  represents the time at which the crack initiates. The vertical dotted line represents the interface. In case of specimen with interface at 42 mm from crack tip (See, Fig. 5.5), two symmetrically propagating daughter cracks can be observed in second layer, whereas, for specimen with interface at 9 mm from crack tip (See, Fig. 5.6), a single crack is observed in the second layer.

## 5.7 Work-in-Progress

The equation for obtaining stress intensity factors from the measured data were formulated during the previous study on dynamic crack propagation reported in [3, 5]. The authors intend to evaluate the SIF histories for all the configurations to establish an empirical relationship between the observed crack growth mechanisms across the interface.

## 5.8 Conclusion

The results indicate that the position of the layer within a PMMA based bi-layer system can alter the crack growth morphology along the interface and in the second layer of an elastically homogeneous bi-layered brittle solid with a plane of weakness oriented normal to the initial crack growth direction. If the interface is positioned very close to the initial crack tip, a crack growth pattern involving single crack is observed in the second layer. Whereas, if the layer is positioned farther away from the initial crack tip, a pattern involving multiple daughter cracks occurs in layer-II. The factors affecting these dramatically different fracture patterns are incident crack velocity and stress intensity factor when impingement on the interface occurs. Further study on investigating these in detail is currently underway.

**Acknowledgment** The authors would like to thank the U.S. Army Research Office for supporting this research through grant W911NF-08-1-0285.

## References

1. Xu, L.R., Huang, Y.Y., Rosakis, A.J.: Dynamic crack deflection and penetration at interfaces in homogeneous materials: experimental studies and model predictions. *J. Mech. Phys. Solid.* **51**(2003), 461–486 (2003)
2. Park, H., Chen, W.: Experimental investigation on dynamic crack propagating perpendicular through interface in glass. *J. App. Mech.* **78**(5) (2011)
3. Kirugulige, M.S., Tippur, H.V.: Measurement of surface deformations and fracture parameters for a mixed-mode crack driven by stress waves using image correlation technique and high-speed photography. *Strain* **45**(2), 108–122 (2009)
4. Periasamy, C., Tippur, H.V.: A full-field digital gradient sensing method for evaluating stress gradients in transparent solids. *Appl. Optics* **51**(12), 2088–2097 (2012)
5. Sundaram, B.M., Tippur, H.V.: Dynamic crack propagation in layered transparent materials studied using digital gradient sensing method. In: *Proceedings of 2014 SEM Annual Conference*, Greenville, SC (2014)
6. Periasamy, C., Tippur, H.V.: Measurement of crack-tip and punch-tip transient deformations and stress intensity factors using digital gradient sensing technique. *Eng. Fract. Mech.* **98**, 185–199 (2013)